CATRINA (2022), 26(1):1-18

Flood Hazard Mapping in Western Luxor, Egypt using Remote Sensing and Spatial Analyses

Mohamed A. Gebril[1*], Maie I. El-Gammal[2], Ahmed M. El-Zeiny[3], Mervat A. El-Sonbati[4]
[1]Geochemical studies Department, central laboratories, Egyptian Mineral Resources Authority (EMRA), Egypt.
[2,4]Environmental Science Department, Faculty of Sciences, Damietta University, Damietta, Egypt
[3]Environmental Studies Department, National Authority for Remote Sensing and Space Sciences (NARSS), CAIRO, Egypt

ABSTRACT

Watershed management is critical to sustainable development. The topographical, and hydrogeomorphological conditions in the western part of the Luxor region give rise to sudden floods. The purpose of the present study is to map the flood hazard zones in the western part of Luxor by using: 1- linear Watershed Index Model (LWIM) through the identification of 24 morphometric parameters; 2- DEM, as input to the GIS environment, using the Arc hydro-Tool; 3- Remote sensing (RS), is built into GIS to detect LU /LC via supervised classification of Landsat images, for the year 1991/2021, and Dreanig density (Dd) maps; 4- Integration of LWIM, Dd, and LU/LC maps. Results indicated that agricultural land increased by approximately (292.7 km^2), while urbanization increased by (43 km^2) between 1991 and 2021, expanding toward the western structure plateau. This study concluded that flood areas west of Luxor are confined to the desert area west of cities Luxor - Arment, and Isna. These areas represent 13.25 % of the hazard flooding zones. The study proposed to establish small dams with diversion channels in the way of the mainstream channels with high orders 4th and directed the water of flood to new canals which joined with the main canals in the study area, re-design of the desert zone west of Luxor.

Keywords: Flash flood hazard; GIS; Hydmorphometric parameters; Luxor; Remote sensing; Topographic hazard.

INTRODUCTION

Flash floods are characterized by rapid occurrence, which can be more difficult to forecast to provide sufficient warning time (Sharma and Mahajan, 2020). Floods often occur in drylands as a result of condensed rainfall, which can damage life and infrastructure as a result of environmental degradation (Abdel-Fattah *et al*., 2017). Construction methods such as ditches, bypass canals, culverts, and ponds are considered easy and effective traditional methods to reduce the risk of sudden flooding. The effectiveness of structural methods depends on the evolution of LU/LC and the monitoring of random development in flood zones. (Kumar *et al*., 2017; Shah *et al.*, 2018). Flood hazard mapping is essential to clarify land use and development in flooded areas where the resulting maps reduce their impact, and sustainable development of the watershed, in addition to protecting against flooding and drought (Abdelkarim *et al*., 2019; Pangali Sharma *et al.*, 2021).

Geomorphological parameters have a direct effect on the potential and danger of flash floods, in addition to topography, climate, geological structures, human processes, drainage systems, and rainfall features. Several researchers have highlighted the relationship between watershed properties and flood impacts (Hassan, *et al., 2012;* Rahmati *et al.*, 2016*;* Jodar-Abellan *et al.*, 2019; Abu El-Magd *et al.*, 2021). Remote sensing studies incorporated in applications for geographical information systems, make it possible to distinguish topographic parameters, hydrogeomorphometric parameters, land cover, and land use, which are beneficial for constructing flood risk models appropriate for the study area (Ebrahimi *et al.*, 2016; Rai 2017; Rana, 2018; Niyazi *et al.*, 2019). Measurable morphometric screening takes into account a variety of linear aspects of the drainage system, such as stream order, stream length, number of streams, and bifurcation ratio. In addition, aerial and relief aspects of the watershed, such as basin relief, relief ratio, ruggedness number, gradient ratio, basin slope, and relative relief, as well as the ground's angle of contribution are considered (Strahler, 1964; Arulbalaji and Padmalal, 2020).

Characteristics of study area

The research area's distinguishing feature can be summed up as being located on the Luxor Governorate on Egypt's western bank of the Nile. The area lies between longitudes 32° 11 and 32° 44 and latitudes 25° 8 and 25° 55 (Figure 1). It is situated in the mid-region between the western desert and the Nile Valley; it is delimited in the west by the limestone Eocene plateau and in the east by the Nile. The geology of the western region of Luxor is characterized by the Late Cretaceous, Paleocene-Eocene, Pliocene, and Pleistocene-Holocene. The terrestrial surface of the region (Figure 2) is characterized by a change in terrain and altitudes, classified by four geomorphological units, the young alluvial plain, the ancient alluvial plain, the eastern structural plateau and the drainage system as described by King *et al.* (2017) and Kamel (2020). Geological and hydrological conditions produce flash floods, where other minor surface runoff with rational probabilities of reloading the existing shallow quaternary aquifer, since 1967. The Aswan Dam has prevented the annual flooding of the Nile, but devastating floods occurred in 1994 which destroyed roads and villages (El- Hosary, 1994; El- Shamy *et al*., 2013). The area is situated in a dry environment, with extreme air temperatures ranging from 22.9°C in January to 40.9°C in July, while the average minimum temperature swings between 5.7°C in January and 23.9°C in July.

* *Corresponding author e-mail:* ***drmohamedaly4@gmail.com***

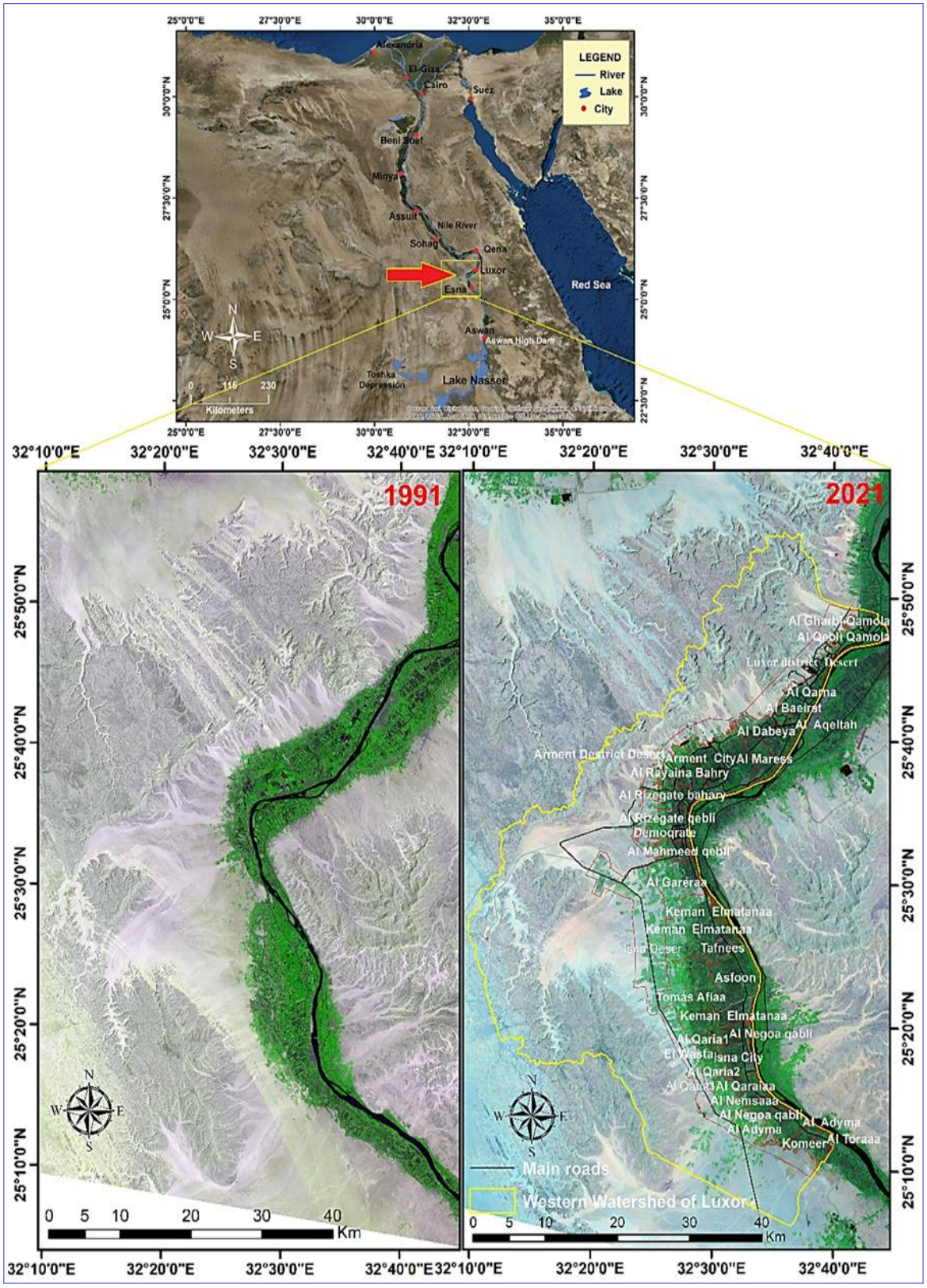

Figure (1): Location map of the study area as retrieved from Landsat images 1991 & 2021 (see Mossad *et al.*, 2022).

Regular monthly relative humidity in the survey area ranges from 25.0% in May to 55.0% in December. The mean monthly wind speed varies in time and location, between 5.9 km/h in October and 9.3 km/h in April. Rainfall is rare and occurs on a random basis throughout the year, with a regular monthly value ranging between 0.0 and 0.3 mm. (Salman *et al*., 2019). Therefore, this study explored the LU/LC and morphometric features to identify the flood risk of sub-watersheds in the western Luxor watershed. A detailed hazard map is presented according to the final hazard degree. This map may serve as a reference for assessing flood mitigation and management.

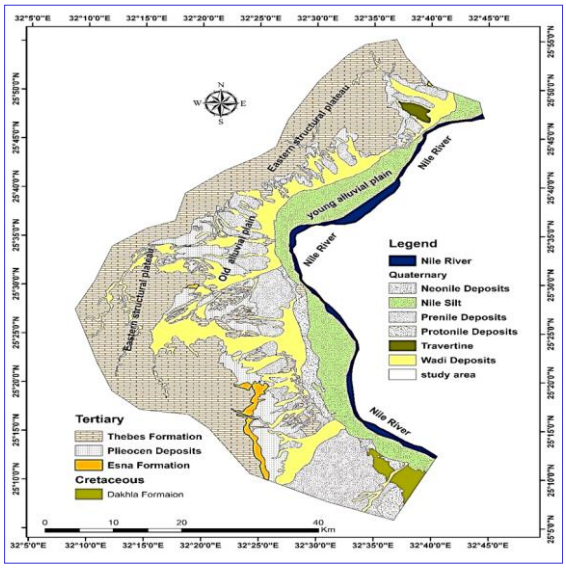

Figure (2): Geological map of the study area, extracted from Map (CONOCO, 1987)

DATA AND METHODS

The designed flow chart summarizes the methodological processes using ArcGIS (ESRI ® ArcMap™ 10.4.1, 2015) and ENVI (ENVI 5.3. 2015) software. The integration between the constructed geospatial mapping data and hydro-morphometric parameters to identify the susceptible flash flood hazard zones in the West Luxor area was clearly diagrammed in Figure (3). Different data and tools had been used as follow: 1, DEM - SRTM (Shuttle Radar Topographic Mission) ~30 m (Figure 4-1, www.usgs.com); 2, Satellite Images for the study area (Landsat-8-OLI/TIRS, 28-4-2021 and Landsat-5-TM, 17-9-1991) (www.usgs.com); 3, Topographic Map (1:50,000, EGSA,2006), and Geologic Maps (CONCO, 1987, 1:500,000 , EMRA, 2006, 1:100000).

Extraction of study area characteristic maps

DEM has been modified using the fill tool (which removes errors such as sinks and removes discontinuity values) in the Arc GIS Hydrology toolset (Figure 2, 4). The main topographic parameters such as contour, slope, aspect, and hill shade maps were extracted by the use of fill-DEM using Arc GIS 3D analysis tools, and topographic and geological maps were obtained from the Egyptian Mineral Resources Authority. The geomorphologic and geological characteristics of the study area were extracted and updated using the digitized tool on the Arc map. The LC/LU changes were derived from Landsat satellite imagery by the integration of RS-ENVI with GIS-Environmental software, through Several steps of the pre-treatment techniques, such as correcting satellite data (UTM) projection type, reference WGS 84, and UTM 36 North area, stacking layers, merging resolution (sharpening), radiometric and atmospheric corrections, and sub-sitting of images. Finally, a supervised classification was conducted to analyze changes in LC/LU. Available geologic, topographic maps, google earth, and field observations are considered when interpreting the images for evolution accuracy. The watershed that affected the study area is illustrated in the workflow process extracted by the Arc-hydro tool. Drainage systems and watersheds were defined and compared to their equivalents on satellite imagery for the evolution of accuracy.

Quantitative morphometric analysis

Using the geomorphometric mathematical equations, GIS software, and the Watershed Modeling System (WMS), 24 geomorphometric parameters were determined based on their direct association with flood hazards (Table 1). These parameters include linear aspect (La), Aerial aspects (Aa), and Relief aspects (Ra).

Flood hazard evaluation

Morphometric parameters were used to control the risk level of dissimilar sub-basins in the western Luxor region. The hazard level of the geomorphometric criterion in each sub-basins area varied between one (lowest hazard level) and five (highest hazard level) (Abdelkarim *et al*., 2019; Pangali Sharma *et al.*, 2021). The level of hazard degree of the geomorphometric criteria was evaluated and computed as follow:

$$HD = \frac{4\,(X - X\,max)}{(X\,min - X\,max)} + 1$$

Where HD, id hazard degree; X, is the value of the geomorphometric criterion of a sub-basin; X_{min} and X_{max} are the lowermost and the major values for the geomorphometric criterion in all drainage sub-basins, respectively; 1,4 are standard values according to references.

The Hazard Degree in the Sub-Basins

The level of hazard in the sub-basins basins was determined in the final stage in two stages:1, the hazards for all geomorphometric criteria were joined into one drainage sub-basin. Five hazard classes were categorized (very high, high, medium, low and very low).

$$HCM = \frac{(\sum mean - \sum min)}{n}$$

Where HCM is hazard class measurements; N_{max} and N_{min} are the maximum and the minimum total sum of the hazard values for one drainage sub-basin, respectively; n, is the number of hazard classes.

Determination of the hazard classes

The first class limit was the lowest total sum of the hazard values for one drainage sub-basin. The second

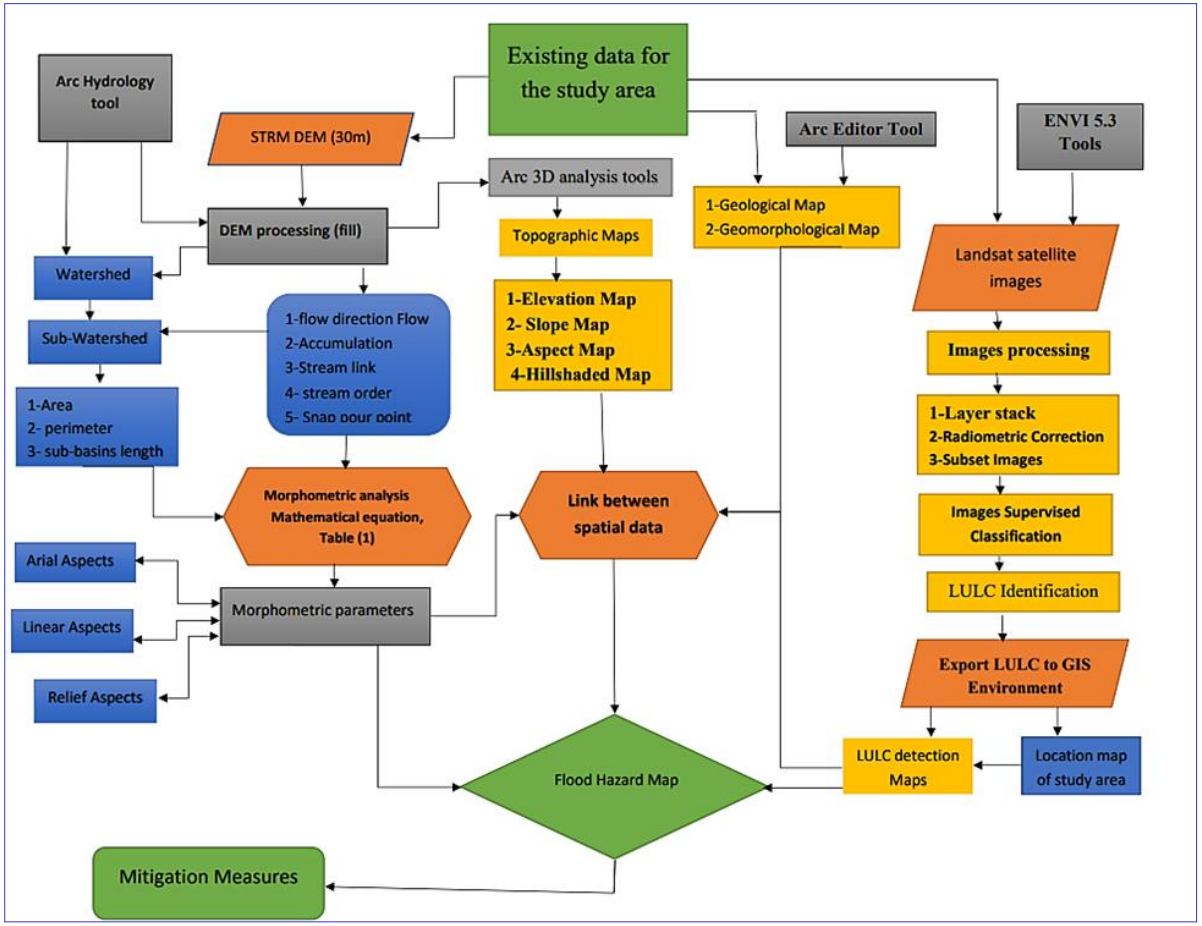

Figure (3): Flow chart showing the flood hazard mapping process in the Western Luxor region**.**

Table (1): Morphometric parameters formula used to identify drainage basins exposed to flood hazards.

Measured parameters	Morphometric Criteria	Method used	Reference
Linear aspects (La)	Stream order (U)	Hierarchical rank	Strahler (1952)
	Number of Streams (Nu)	Nu= N1+N2…+N6	Horton (1945)
	Stream length in km (Lu)	Lu= L1+L2….+L6	Horton (1945)
	Bifurcation Ratio (Rb)	Rb = Nu/Nu+1	Schumm(1956)
	Weighted mean bifurcation ratio	WMRb = P (Rbu/Rbu + 1)/(Nu + Nu + 1)/ P N	Strahler (1957)
	Stream length Ratio (RL)	RL = Lu / Lu-1	Horton (1945)
Areal aspects (Aa)	Area in km^2 (A)	GIS software analysis	Schumm (1956)
	Perimeter in km (P)	GIS software analysis	Schumm (1956)
	Length of basin in km (L_b)	GIS software analysis	Schumm (1956)
	Drainage density (Dd)	Dd = ∑Lu /A	Horton (1932)
	Stream frequency (Fs)	Fs = Nu/A	Horton (1932)
	Circulatory ratio (Rc)	Rc = 12.57*(A/P²)	Miller (1953)
	Elongation ratio (Re)	Re = 2/ Lb *√(A /π)	Schumm (1956)
	Form factor (Ff)	Ff = A/Lb²	Horton (1932)
	Texture ratio (T)	T = Nu/P	Horton (1945)
	Drainage intensity (Di)	Di = Fs/Dd	Faniran (1968)
	Mean Basin Width (Wb)	W_b=A/L	Horton (1932)
	Relative perimeter (Pr)	P_r= A/P	Schumm (1956)
	Constant channel maintenance (C)	C=1/Dd	Schumm (1956)
	Lemniscate ratio (k)	K=L_b^2/4A	Chorley (1957)
	Wandering ratio (Rw)	Rw=C_l /Lb	Smart&Surkan (1967)
	Compactness coefficient (Cc)	Cc=0.2841 P/A $^{0.5}$	Horton(1945)
	Sinuosity index (S_i)	S_i = C1/V1	Muller (1968)
	Topographic sinuosity index (Tsi)	Tsi = V1 − 1/C1 − 1 × 100	Muller (1968)
Relief Aspects (Ra)	Basin relief in m (H)	H = Z - z	Strahler (1957)
	Relief ratio (Rr)	Rr = H / Lb	Schumm (1956)
	Relative Relief (ReRe)	ReRe = H*100 / P	Melton(1957)
	Ruggedness number (Rn)	Rn= Bh× Dd	Schumn, 1956
	Gradient ratio (Rg)	Rg= (Z - z) /Lb	Sreedevi et al. (2005)
	Hypsometric integral (HI)	$HI = \frac{(H\ mean - H\ min)}{(H\ max - H\ min)}$	Muller (1968)

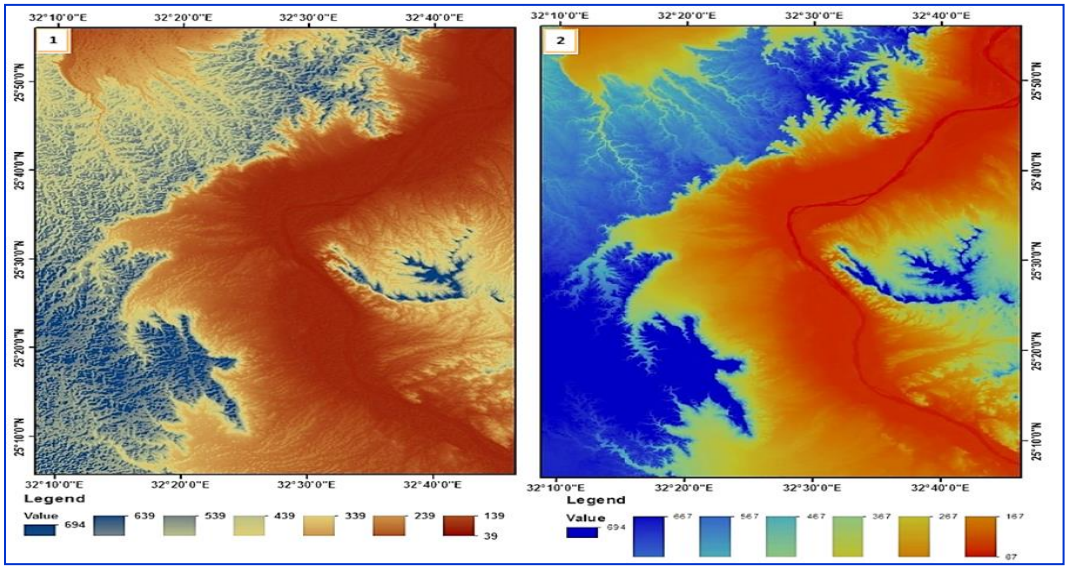

Figure (4): Satellite of the study area. 1, SRTM image; 2, Filled SRTM image.

class limit was the sum of the lowest sum of hazard values for a drainage sub-basin and the width of the hazard class. The additional hazard modules were controlled by repeating same technique. The final phase was deriving the overall risk category values within the five hazard degree.

RESULTS AND DISCUSSION

The results of this study demonstrated that there is a very high risk of flash floods in the evaluation of the watershed of the western Luxor area by combining three methodologies; linear mathematical equations of flood model index with 24 morphometric factors, and GIS computability with RS.

LULC Maps

Detection of changes in LULC indicated that the study area is divided into five categories: water, agriculture, sand dunes, urban, and rocky areas. The results of the LULC analysis as illustrated in figure (5) indicate a significant increase in agricultural activities and urban expansion from 1991 to 2021. Agricultural land increased by 292.7 km^2, while urbanization increased by (43 km^2) between 1991 and 2021. The tendency of agriculture and urban development to the east, where the high plateau of the geological structure, thus the new urbanization and reclamation land in danger of flooding. The LULC map indicated that the expansion of the urban and agricultural area through uncontrolled planning led to changes in the study area's hydrographic and hydrological system which may lead to urban flooding during heavy rainfall (Kamel, 2020; Pangali Sharma *et al*., 2021).

Topographical parameters

The DEM has been classified into eight zones, for the elevation map, the maximum altitude is close to 610m in the west, where the structural plateau of the western Luxor region (dissected plateau with its hydrographic system), while the minimum elevation is 69 m in the outlet of the sub-basins. Figure (6) showed the elevation, slope, Hill shade, aspect maps of the study area. The slope map demonstrates that the slope decreases from west to east and north to south, with a degree of slope of 0-120 (low slope), moderate slope (13-250), and a high slope (26-740). The slope faces are directed towards the east, followed by the north, the anterior part of the study area characterized by flat soils. The hill-shaded map is indicated the smooth topography in the eastern part of the study area (alluvial plain) while the geomorphic units located in the west and the north-west are highly dissected, topographical maps. Topographical features revealed that the flat earth is small compared to the rising area, in addition to the main direction of the slope to the east which indicates a flat area in danger of flooding. Figure (7) shows the western structural plateau elevation in the study area.

Quantification of morphometric parameters

The DEM analysis indicated that the study area contains 34 sub-basins of different sizes, as illustrated in Figure (8).

Linear aspects

Stream order system (U), has been tabulated according to Strahler's (1952) model as shown in Table (1). Sub-basins recorded 6^{th} orders ranged between the largest sub-basins (6^{th}) to the smallest sub-basins (2^{nd}). The total number of streams (Nu) for sub-basins of the study area recorded as 5335 streams for sub-basins, 4151streams are linked up to the 1^{st} order, 902 streams are linked up to the 2nd order, 210 streams are linked up to the 3^{rd} order, 55 streams are linked up to the 4^{th} order. In addition, 14 streams are linked up to the 5^{th} order and 3 streams are linked up to the 6^{th} order. Meanwhile, stream length (Lu), which reported as the total extent of streams, recorded 4832.96 km that declines with growing stream order, with the highest values 2379.28, 1214.23, 666.43, 387.73, 142.45, and 42.84 km streams are linked up to the 1^{st}, 2^{nd}, 3^{rd}, $4th$, 5^{th}, and 6^{th} order, respectively. Greater slope area and finer surfaces have smaller stream extents. On the other hand, extended streams' lengths designate flatter gradients, the direction of the mainstream to east and east-north (Asfaw and Working, 2019).

Bifurcation ratio (Rb)

It is the important morphometric parameters that reflect the basin geometry and its geological structure. In light of this, the value represents the basin's potential for water flow. According to Table (2), the majority of Rb values at the west Luxor sub-basins typically have values between 2 and 5, indicating that geological components do not disturb the drainage pattern (Joji *et al*., 2013). Six sub-basins, each referencing the typical drainage pattern seen in a typical rock, have values ranging from 3 to 5. Other sub-basins have values in the range of 2-3, remarking that the sub-basins have degraded from less severe structural deterioration and highlighting flat areas. In sub-basins with lower Rb values, damage and flood hazard are observed to increase locally rather than over the entire basin (Tesema, 2021; Strahler, 1964).

Sinuosity Index (Si).

Si is a marker for geologic structure, erosion, and runoff rate. The Si values recorded, for the study sub-drainage areas, were ranged from 1.08 to 1.76, as shown in Table (2). A higher number denotes a low geologic structure, a strong pace of erosion, and a low rate of meandering (Khare 2014).

Topographic Sinuosity Index (TSi)

Due to the significance of TSi, which defines the stage of river basin development with respect to natural stream flow and development flood plain, this factor was taken into account. The sub-basins in the research area had TSi values ranging from 33.33% to 87.5% (Table 2). The sinuosity analysis makes it clear that the values of TSi are either at or close to the value of 60% due to developing topographic limits on the channel in this area of the alluvial plain (Mueller, 1968; Malik and Pal,2020).

Arterial aspect

Form factor (Ff)

The ratio of basin area to the square of basin length is termed as the form factor (Horton 1932). It varies

from zero, which considered a highly elongated shape, to one, which is considered a perfect circular shape (Pareta and Paret, 2011; Choudhari *et al*., 2018). It is clear from Table (2) that the largest sub-basins in the study area have a low (Ff) value ranged from 0.13 to 0.54, signifying the elongation in their shape. However, sub-basins B14, B21, B28, and B31and B33 that have high values ranged from 0.76 to 1.54 that display circular shape are considered exception. Flood flows of such elongated basins are easier to be managed than those from circular basins (Farhan *et al*., 2016).

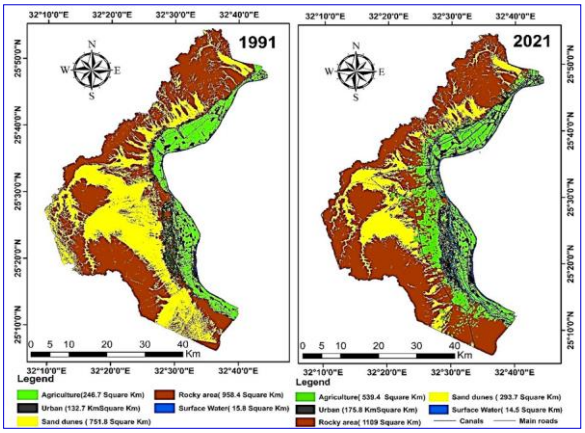

Figure (5): LULC maps produced by supervised classification techniques, area of LULC classes as a percentage of all landscape classes between 1991 and 2021.

Circularity ratio (Rc).

Rc is the ratio of the basin's surface area to the surface area of a circle having a radius between 0.4 and 0.5 and a perimeter equal to the basin's (Miller, 2003). The value of Rc is a dependable indicator for determining the drainage discharge of sub-basins during a flooding season (Jha, 1996). In our study area, the RC values ranged from 0.00 to 0.34 and indicate sub-basins with tributaries in the youth stage, sub-basins that are not circular but rather more elongated in shape, low runoff, which allows for ample time for water infiltration and indicates that the subsoil condition is highly permeable, and structural instability cont-rolled by drainage systems (Kuntamalla *et al*., 2018).

*Elongation ratio (Re***)**

The ratio of the diameter of the circle in the drainage basin's area to the basin's longest possible length is known as Re (Schumm, 1956). The value of the elongation ratio ranges from 0.6 to 1.0. (Strahler, 1952). All sub-basins in the research area have elongation ratio values less than 0.5, indicating more outline elongation, while sub-basins B14, B21, B28, and B33 have elongation ratio values ranged between 0.5-0.70, indicating elongation shape (Biswas, 2016; Rai, 2019).

Drainage density (Dd)

It has also been demonstrated that the basin with the highest stream density and drainage is most susce-ptible to flooding. Dd is thought to indicate the runoff and discharge condition of a basin (Horton, 1932). The majority of the sub-basins in the study area (Table 2)

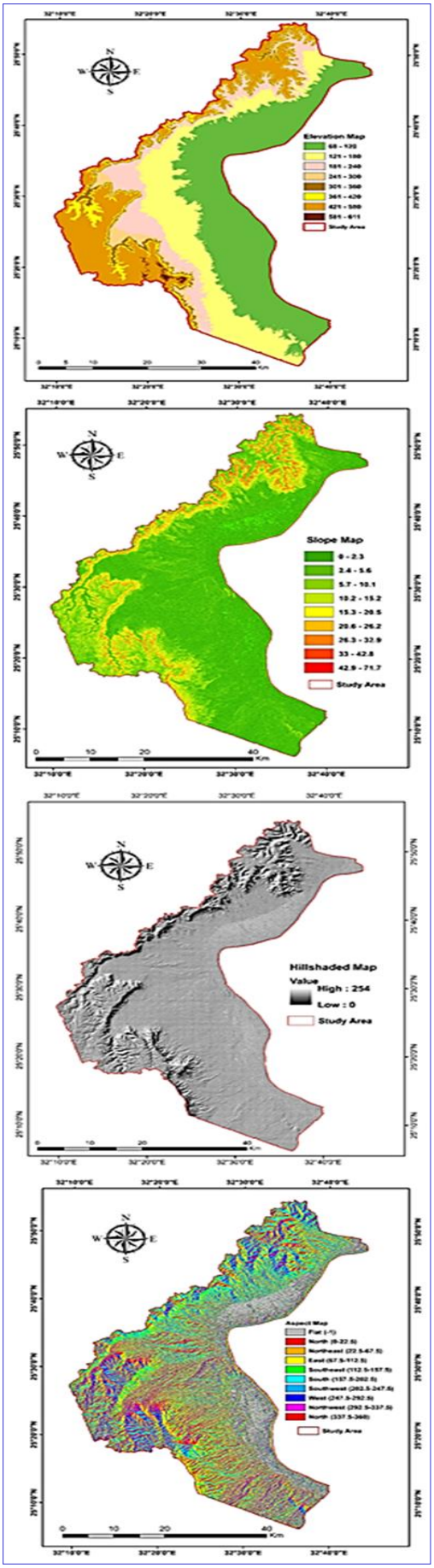

Figure (6): Elevation, slope, Hill shade, and aspect maps of the study area**.**

Table (2): The values of the geomorphometric characteristics of the drainage sub-basins influence the west Luxor area.

Sub-basin	Hazard Degree†																							
	Direct impact													Indirect impact										
	A	Lb	Nu	Rc	Fs	Dd	Si	Rg	Wb	Pr	H	Rr	ReRe	Rn	Rb	Re	Rf	T	Tsi	WM Rb	Cc	Rw	HI	K
B1	539.48	45.00	1292.7	0.30	2.45	2.40	1.31	0.01	11.54	3.60	0.53	0.36	0.01	1.28	3.40	0.29	0.27	8.83	76.09	4.56	1.83	1.01	0.37	0.94
B2	432.37	53.43	1002.8	0.16	2.71	2.32	1.68	0.03	10.49	2.31	0.50	0.27	0.01	1.16	3.45	0.22	0.15	6.27	59.09	4.33	2.55	1.63	0.48	1.65
B3	340.91	40.41	783.94	0.15	3.16	2.30	1.57	0.03	9.47	2.02	0.54	0.32	0.01	1.25	4.45	0.26	0.21	6.37	63.04	5.57	2.60	1.31	0.48	1.20
B4	244.88	21.76	612.45	0.34	1.97	2.50	1.34	0.02	8.21	2.56	0.44	0.46	0.02	1.09	2.77	0.41	0.52	5.06	73.57	3.65	1.73	0.97	0.47	0.48
B5	116.56	25.00	239.11	0.05	2.17	2.05	1.56	0.07	5.95	0.69	0.44	0.26	0.02	0.90	3.00	0.24	0.19	1.50	63.07	4.01	4.45	1.61	0.50	1.34
B6	116.33	22.00	291.38	0.07	2.30	2.50	1.49	0.07	5.95	0.78	0.51	0.34	0.02	1.27	3.06	0.28	0.24	1.79	66.24	4.30	3.94	1.66	0.38	1.04
B7	72.74	19.50	168.64	0.04	2.54	2.32	1.50	0.10	4.86	0.46	0.15	0.09	0.01	0.34	2.92	0.25	0.19	1.18	65.20	4.65	5.24	1.74	0.45	1.31
B8	39.11	17.50	87.12	0.03	2.71	2.23	1.27	0.16	3.71	0.33	0.13	0.11	0.01	0.28	3.33	0.20	0.13	0.88	77.89	5.05	5.44	1.90	0.47	1.96
B9	32.16	12.70	69.35	0.05	3.08	2.16	1.42	0.15	3.41	0.37	0.44	0.52	0.03	0.96	2.51	0.25	0.20	1.15	68.31	4.50	4.32	1.61	0.49	1.25
B10	26.77	14.20	57.63	0.02	2.80	2.15	1.48	0.22	3.15	0.21	0.44	0.35	0.03	0.96	5.47	0.21	0.13	0.58	65.63	6.87	7.04	2.00	0.48	1.88
B11	17.74	9.20	39.12	0.03	3.21	2.21	1.29	0.22	2.64	0.19	0.06	0.07	0.01	0.14	2.85	0.26	0.21	0.61	75.26	4.12	6.28	1.59	0.52	1.19
B12	16.77	8.50	38.17	0.03	2.80	2.28	1.31	0.23	2.58	0.21	0.43	0.54	0.05	0.97	2.63	0.27	0.23	0.59	73.68	4.28	5.51	1.61	0.48	1.08
B13	8.34	6.80	19.47	0.02	2.88	2.34	1.24	0.38	1.91	0.12	0.40	0.56	0.06	0.94	1.93	0.24	0.18	0.34	77.94	2.93	7.04	1.78	0.42	1.39
B14	6.07	2.40	13.92	0.02	3.13	2.29	1.76	0.43	1.66	0.09	0.32	0.46	0.13	0.74	2.17	0.58	1.05	0.27	48.00	4.35	8.10	1.64	0.37	0.24
B15	5.56	3.20	12.08	0.00	3.42	2.17	1.19	0.35	1.60	0.04	0.01	0.01	0.00	0.03	2.67	0.42	0.54	0.15	79.41	4.64	15.45	1.27	0.44	0.46
B16	5.25	4.80	13.35	0.00	3.62	2.54	1.28	0.47	1.56	0.04	0.02	0.02	0.00	0.05	2.67	0.27	0.23	0.15	73.33	4.64	15.90	1.63	0.54	1.10
B17	4.65	5.20	8.93	0.01	1.94	1.92	1.45	0.67	1.48	0.05	0.03	0.03	0.01	0.05	4.00	0.23	0.17	0.09	63.79	8.00	13.03	2.17	0.53	1.45
B18	4.27	5.60	9.59	0.03	2.11	2.25	1.40	0.68	1.43	0.11	0.33	0.80	0.06	0.73	1.70	0.21	0.14	0.22	66.07	2.73	5.56	2.21	0.39	1.84
B19	3.69	3.20	8.41	0.01	3.26	2.28	1.41	0.48	1.34	0.06	0.02	0.03	0.01	0.04	2.17	0.34	0.36	0.19	60.71	3.96	3.80	1.38	0.57	0.69
B20	3.65	3.00	8.07	0.02	3.56	2.21	1.20	0.42	1.33	0.07	0.02	0.04	0.01	0.04	2.00	0.36	0.41	0.24	76.09	3.00	8.17	1.21	0.42	0.62
B21	3.08	1.50	7.50	0.00	1.62	2.44	1.38	0.74	1.24	0.03	0.07	0.07	0.04	0.16	2.00	0.66	1.37	0.05	64.85	4.00	16.02	1.88	0.51	0.18
B22	2.83	3.70	6.22	0.00	2.12	2.20	1.19	0.61	1.19	0.03	0.06	0.06	0.02	0.14	2.50	0.26	0.21	0.06	78.00	5.00	16.71	1.48	0.45	1.21
B23	2.70	3.00	5.98	0.00	2.97	2.22	1.48	0.74	1.17	0.03	0.02	0.02	0.01	0.05	1.50	0.31	0.30	0.08	56.67	2.35	17.12	1.74	0.52	0.83
B24	2.15	2.50	4.34	0.01	3.26	2.02	1.60	0.75	1.06	0.04	0.01	0.03	0.01	0.03	1.33	0.33	0.34	0.13	45.45	2.00	10.54	1.58	0.49	0.73
B25	2.10	3.00	4.08	0.00	2.86	1.94	1.08	0.64	1.05	0.02	0.01	0.01	0.00	0.01	2.50	0.27	0.23	0.06	87.50	5.00	19.40	1.30	0.39	1.07
B26	1.72	2.50	3.44	0.00	2.91	2.01	1.20	0.74	0.96	0.02	0.06	0.06	0.02	0.12	2.00	0.30	0.27	0.05	71.43	4.00	21.44	1.35	0.48	0.91
B27	1.63	3.60	4.80	0.00	1.84	2.95	1.22	1.08	0.94	0.02	0.05	0.05	0.02	0.16	1.00	0.20	0.13	0.03	73.91	2.00	22.03	1.91	0.51	1.99
B28	1.54	1.00	3.27	0.00	3.25	2.12	1.33	0.56	0.92	0.02	0.02	0.02	0.02	0.03	2.00	0.70	1.54	0.05	33.33	4.00	22.65	0.95	0.44	0.16
B29	1.49	2.50	3.64	0.00	3.35	2.44	1.38	0.80	0.91	0.02	0.02	0.02	0.01	0.04	2.00	0.28	0.24	0.05	50.00	4.00	23.00	1.34	0.45	1.05
B30	1.32	2.20	3.57	0.00	3.79	2.71	1.19	0.79	0.86	0.01	0.01	0.01	0.01	0.04	2.00	0.29	0.27	0.05	66.67	4.00	24.47	1.24	0.46	0.92
B31	1.28	1.30	2.36	0.00	3.12	1.84	1.25	0.65	0.85	0.01	0.02	0.02	0.01	0.03	1.50	0.49	0.76	0.04	40.00	3.00	24.83	0.99	0.50	0.33
B32	1.19	2.00	2.96	0.00	3.35	2.49	1.19	0.89	0.82	0.01	0.02	0.02	0.01	0.05	1.50	0.31	0.30	0.04	66.67	3.00	25.73	1.31	0.57	0.84
B33	1.08	1.00	1.99	0.00	4.65	2.26	1.36	1.00	0.79	0.01	0.02	0.02	0.02	0.05	2.00	0.59	1.08	0.05	44.44	4.00	27.09	1.39	0.51	0.23
B34	1.07	1.70	2.59	0.00	4.65	2.01	1.21	0.90	0.79	0.01	0.02	0.02	0.01	0.03	2.00	0.34	0.37	0.05	57.14	4.00	27.10	1.24	0.49	0.67

† Meanings of the letters A, Lb, Nu, Rc, Fs, Dd, Si, Rg, Wb, Pr, H, Rr, ReRe, Rn, Rb, Re, Rf, T, Tsi, WMRb, Cc, Rw, HI, and K as they are listed in the table (1)

ranged from 1.84 to 2.95 km/km^2, which indicates smooth to high slope to large sub-basins, resistant rocks, weak impermeable subsurface material with condensed vegetation cover, and abrasive texture. Large sub-basins within the study area are more exposed to flood risk than small basins (Choudhari *et al.*, 2018; Abdul Qadir *et al.*, 2020).

Stream frequency (Fs)

Fs represents the total number of streams for all orders in a given location (Horton, 1945). The lithology of the basin and the vegetation cover affect (Fs) value. A hard rock structure and penetrable subsurface material were both suggested by small values of Fs (Reddy *et al.*, 2002). The sub-basins in the study area had high (Fs) values of 1.62-4.65 (km^2), indicating that they are not flat and have a high relief as well as nonpermeable subsurface materials (Ali *et al*., 2018).

Constant channel maintenance (C)

C is a crucial variable that reflects drainage density's inverse (Malik *et al*., 2020). Low C values for sub-basins in the study area, ranged from 0.34 to 0.54km^2/km as reported in Table (2), indicating weaker or less resistant soils, scant vegetation, and stony topography.

Mean Basin Width (Wb)

The separation line defines the beginning and end of the branch and Wb give a good idea of the allowable extent of the branches in the basin. Sub-basins in the research region drainage have values ranged between 0.78 and 11.45, suggesting that they are rectangular in shape and have a higher elongation ratio (Pareta *et al*., 2011).

Lemniscate Factor (K)

In order to define the geometrical characteristics of drainage basins, we can employ the lemniscate factor (K), which is the ratio between the square of the basin length and four times the size of the basin. Since the K factor of the drainage sub-basins, of the study area, ranges from 0.16 to 1.99, it is clear that the water systems on dip slopes are predominantly elongated in shape (Ivanova *et al*., 2012).

Wandering ratio (Rw)

Rw is defined as the proportion of mainline length to basin length (Gabale *et al*., 2015). The Rw values for the sub-basins ranges from 0.95 to 2.22, as indicated in Table (2).

Compactness Coefficient (Cc)

The ratio Cc is the distance between the basin's circumference and a circle whose area is the same as the basin's drainage area. According to Table (2), the Cc values vary from 1.73 to 27.10. The high value of Cc indicated the sub-basins' regular shape in the research region and their ability to flood (Iqbal, 2014).

Relief Aspects parameters

Basin relief (H)

The elevation difference between the watershed's highest point (Z) and lowest point (z) is measured and represented as H (Strahler, 1957). The importance of H is to control the stream gradient and affect the surface runoff and sediment (Choudhari *et al*., 2018). The research area's relief was lowered from south to west indicating that the runoff path was from west to east to north (Table 2).

Figure (7): Field photographs that display the western structural plateau's height in the research area.

Relief ratio (Rr)

Rr is the ratio of the length of the major drainage line to the whole length of the basin's relief (Schumm, 1956; Rai *et al*., 2018). The sub-basins exhibit Rr values ranged from 2.33 to 133 m/km, as reported in Table (2). While high values indicate greater slope and less permeability of the subsurface, low values of Rr are caused by a low degree of gradient (Rai *et al*., 2017a & 2017b).

Relative relief (ReRe)

ReRe is the most dynamic component of the morphometric variable that is used to evaluate the overall morphology of terrain faces and segmentation gradation. The lower values of study area (Table 2) represent basin exposure to flood dangers, flat ground,

and a gradual slope close to the sub-basins' outlets (Tesema *et al.*, 2021).

Ruggedness number (Rn)

Extreme basin relief and drainage density result in Rn, which typically combines length and slope gradient. Rn describes the likely consequences of drainage density, slope steepness, and soil erosion on the landforms (Strahler, 1968). According to the table (2), the Rn values for sub-basins ranged from 0.01 to 1.28. Due to their channel gradient, peak discharge, and dissection, high-roughness sub-basins have a potential of flooding (Singh *et al*., 2020).

Gradient ratio (Rg)

Rg is a parameter of channel slope facilitated analysis of the runoff volume (Sreedevi *et al.*, 2005). The values of Rg for the sub-basins were varied and ranged from 0.01 to 1.08, indicating moderate to high relief terrain with the main channel flowing in gently sloping terrain (Iqbal, 2014).

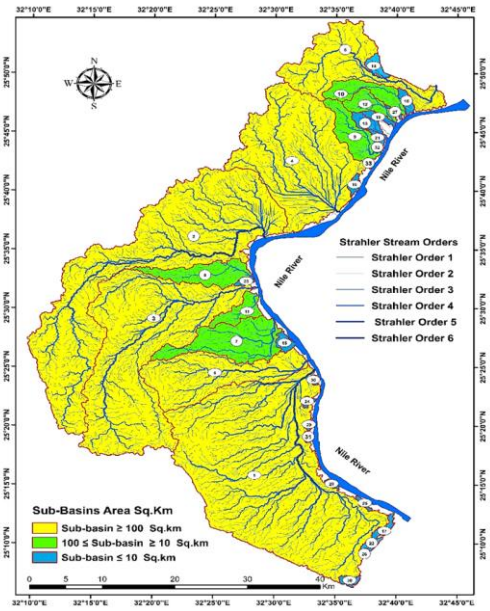

Figure (8): Aspect map of the study area, western Luxor, showing the western structural plateau elevation and sub-basins delineation.

Hypsometric analysis of sub-basins

Due to the fact that the variance in size is not interpreted as overlapping during analysis, the hypsometric examination is a dimensionless parameter useful for evaluating watersheds (Strahler, 1952). In addition, it provides a significant amount of useful data regarding the erosion stage of the basin corresponding with the land elevation, tectonic activity, climate change, and lithological changes. Consequently, it helps with environmental monitoring, which facilitates basin planning and organisation (Duan, *et al.*, 2022).

Hypsometric Integral (HI)

The hypsometric integral defines a time scale that represents a phase in which the rivers' wadis move. According to Table (2), the hypsometric integral values vary from 0 to 1 (Muller, 1968; Andreani *et al*., 2014). The erosion cycle, which is the total length of time needed to bring a land topological unit to its base level, can be calculated using the indicator HI. Each of its three subcategories corresponds to one of the geomorphic cycle's three distinct phases. These are categorized as following: i, The old stage if HI≤0.35, in which the basin is fully stabilized; ii, the complete stage is 0.35≤ HI ≤0.60, which means the basin growth has attained a steady-state disorder and iii, in the early stage if HI ≥0.60, where the basin is highly liable to erosion and is under expansion (Shivaswamy, et al., 2019). As shown in Table (2) the values of HI, for sub-basins in the study area varied between 0.37 and 0.57 indicating that 34 sub-basins in the study area belong to the mature stage of moderated erosion, not affected by tectonic or geological disturbance (Gharehchahi *et al*., 2021).

Matrix Correlation

The correlation matrix indicates the relationship among morphometric parameters. There are about 300 correlations between the 24 geomorphometric variables. Figure (9) illustrated the percentage of the relationship coefficient between hydromorphometric variables based on the value of (R_2). Au, Lb, Nu, Rc, Dd, Wb, Pr, H, Rn, Rb, T, Tsi, WMRb, and K are positively related to most other variables, while Fs, Si, Rg, Rr, ReRe, Re, Rf, Cc, Rw, and HI are negatively related to most other variables.

Flood Hazard Map of the study area

Application of linear equations for the direct and indirect effects of morphometric characteristics proved effective for the morphometric parameters of the study area sub-watershed used for WMS and a flood hazard modelling. Flood hazard was classified into five groups, ranging from very low to very high, using the the hazard degree weighted values (Table 3) and flood hazard index (Table 4). The calculated morphometric values were clustered in five different weights. Flood danger zones are from 1 to 5. Table (5) shows that the drainage sub-basins have extremely high, high, medium, low, and very low hazard levels. These drainage sub-basins represent an area of approximately 1557.64 km^2, 116.33 km^2, 184.16 km^2, 138.39 km^2, and 65.83 km^2, respectively. This means that 76% of the study area is subject to structural hazards that increase the risk of flooding. The overall flood potential risk map was created by giving hazard values to the specific sub-basins (Figure 10A).

Flood Hazard Map interpretation

Although flood maps indicate flooding, no flooding has occurred since 1994, sub-basins 1, 2, 3, and 4 fall into the very high class while sub-basin 6 fall into the high flood hazard, A very high-risk sub-basin 1, 2, 3 and 4 might not be entirely exposed to floods. Therefore, detailed risk identification was necessary to examine flash flood potential risk per Km^2 pixel using drainage density, and slope, so in compiling the drainage density and slope with LULC maps, the present study detected the zone of the pocket at risk due to flash flooding (Figure 10B).

LULC map of the watershed of the study area indicates a significant increase in agricultural activities

and urban expansion. Agricultural land increased by approximately (239.4 km^2), compared to (175.8 km^2) for separate populations, villages, and cities. Integrated slop, flood The LULC map indicated, that the study area has a good network of canals that reduces the impact of flood risks and the hydrographic system. the channels are used to collect the water and direct it to the water channels and the excess is direct to the Nile.

Agriculture and urban expansion proceed through random plans that deform the watershed system. In addition, flooding risks have been confined to the desert area west of the study area, where the high plateau of the geological structure is located. Therefore, a new urban and agricultural area can be flooded, especially in the areas between the cities of Luxor Arment and the cities of Arment- Isna. This means that flooding may be confined to specified zones, not all study areas as illustrated in Figure (11). Effective Mitigation measures include structural solutions such as detention dams, cisterns, and mitigation canals (Figure 11).

CONCLUSION

The watershed of the western Luxor region was assessed using three methods including linear mathematical equations of flood model index with 24 morphometric factors and GIS computability with RS. The data obtained revealed that the main direction of flow is east, north, and northeast. The watershed of western Luxor is divided into 34 sub-basins that vary in their shape and size. According to DEM and morphometric analysis, basins 1, 2, 3, and 4 are the largest sub-basins in the study region and are at extremely high risk of flash floods, while basin 6 is in the high zone. An integrated flood map that includes slop, drainage density, and LULC maps was used to identify a new urban and agricultural area as being at risk of flooding. This area is especially located in the west desert zones between the cities of Luxor Arment and the cities of Arment-Isna. Government oversight and management of development in these zones are therefore necessary. Urban flooding may occur during periods of high rainfall due to changes in the hydrographic and hydrolytic system caused by the unregulated expansion of the urban and agricultural zones west of the Luxor watershed. The government must take notice and exercise coordinated plans of control over it. The current findings can serve as a starting point for designing land use and flood control projects in the western Luxor region. For mitigation measures, LULC integrated with the final flood map illustrated that the eastern part of the study area is at more risk to elevation and many streams of high order 4th, 5th, 6th which transport a great volume of water. Therefore, establishment of small dams with diversion channels in the way of the mainstream channels with high orders 4th, 5th, 6th are suggested. Also, new communities must be controlled and managed by governments through planned projects and laws. Re-planning and organizing the random urban and redirecting the flood stream by alleviation canals that located in the hazard zones.

REFERENCES

ABDEL-FATTAH, M., SABER, M., KANTOUSH, S.A., KHALIL, M.F., SUMI, T., SEFELNASR, A.A., 2017, Hydrological and geomorphometric approach to understanding the generation of Wadi Flash Floods. Journal of Water, 9 (7): 553.

ABDELKARIM, A., GABER, A.F.D., YOUSSEF, A.M., PRADHAN, B., YOUSSEF, A.M.,2019, Flood Hazard Assessment of the Urban Area of Tabuk City, Kingdom of Saudi Arabia by Integrating Spatial-Based Hydrologic and Hydro-dynamic Modeling. Journal of Sensors, 19(5):10-24.

ABDUL QADIR, MOHAMMAD YASIR, ISMAIL AHMAD ABIR, NASEEM AKHTAR, LIM HWEE

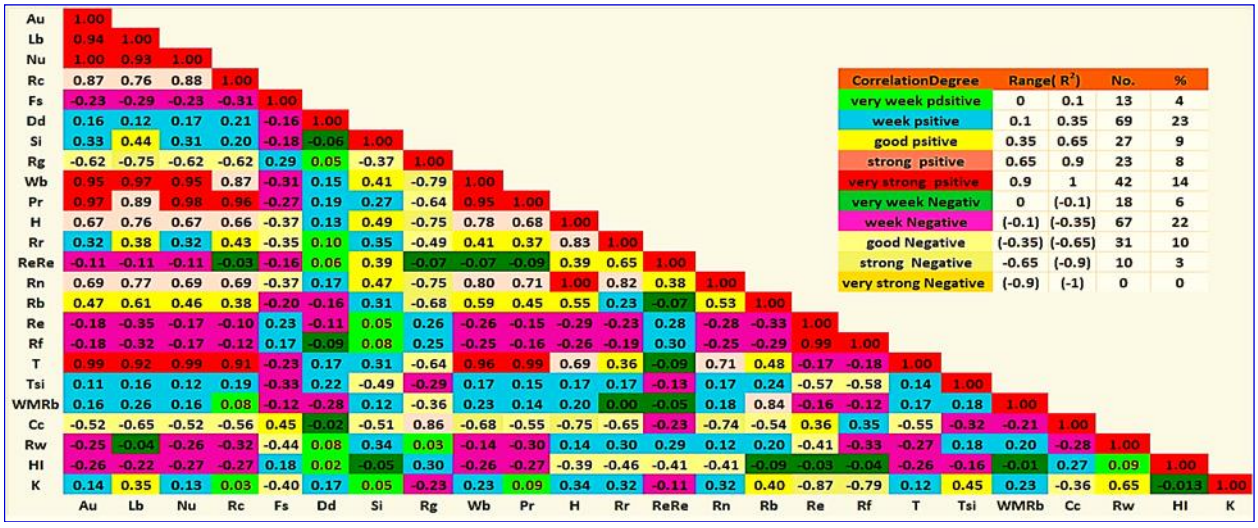

Figure (9): Correlation matrix of calculated morphometric parameters in the study area.

Table (3): Ranks for the geomorphometric weighted values of the influence of drainage sub-basins in the western Luxor area.

Sub - basin	Hazard Degree†																							Total
	Direct impact													Indirect impact										
	A	Lb	Nu	Rc	Fs	Dd	Si	Rg	Wb	Pr	H	Rr	ReRe	Rn	Rb	Re	Rf	T	Tsi	WMRb	Cc	Rw	HI	K	
B2	4	5	4	3	3	4	5	1	5	5	5	2	1	4	3	5	5	1	3	3	5	3	2	2	83
B3	3	4	3	3	5	4	5	1	5	5	5	2	1	5	2	4	5	1	2	2	5	4	2	1	79
B4	2	2	3	5	2	4	3	1	4	5	4	3	1	3	3	3	4	2	1	3	5	5	2	5	75
B5	2	2	2	1	2	3	5	1	4	4	4	2	1	3	3	5	5	3	2	3	5	3	2	2	69
B6	2	2	2	1	2	4	4	1	4	4	5	2	1	5	3	4	5	3	2	3	5	3	3	2	72
B7	1	2	2	1	2	4	5	2	4	4	1	1	1	1	3	4	5	3	2	2	5	2	2	2	61
B8	1	2	2	1	3	3	2	2	3	4	1	1	1	1	3	5	5	4	1	2	5	2	2	2	58
B9	1	1	2	1	3	3	4	2	3	4	4	4	1	3	2	4	5	3	2	2	5	3	2	3	67
B10	1	2	1	1	2	3	4	2	3	3	4	2	1	3	1	5	5	4	2	1	4	1	2	2	59
B11	1	1	1	1	3	3	2	2	3	3	1	1	1	1	3	4	5	4	1	3	4	3	1	3	55
B12	1	1	1	1	2	3	3	2	3	3	4	3	3	3	3	4	5	4	1	5	5	3	2	3	68
B13	1	1	1	1	2	3	2	2	3	3	4	4	4	3	5	4	5	5	1	4	4	2	2	3	69
B14	1	1	1	1	3	3	5	3	3	2	3	4	5	2	5	2	2	5	4	3	4	3	3	5	73
B15	1	1	1	1	3	3	1	2	3	2	1	1	1	1	3	3	4	5	1	2	3	4	2	5	54
B16	1	1	1	1	4	4	2	3	3	2	1	1	1	1	3	4	5	5	1	2	3	3	1	4	57
B17	1	1	1	1	1	2	5	4	2	2	1	1	1	1	5	5	5	5	2	1	3	1	1	3	55
B18	1	1	1	1	1	3	4	4	2	3	3	5	4	2	5	5	5	5	2	5	5	1	3	2	73
B19	1	1	1	1	3	3	4	3	2	2	1	1	1	1	5	4	4	5	2	3	4	4	1	5	62
B20	1	1	1	1	4	3	2	3	2	2	1	1	1	1	5	4	4	5	1	2	4	4	2	5	60
B21	1	1	1	1	1	4	3	5	2	2	1	1	2	1	5	1	1	5	2	3	3	2	1	5	54
B22	1	1	1	1	1	4	1	4	2	2	1	1	1	1	5	4	5	5	1	2	3	4	2	2	55
B23	1	1	1	1	2	4	4	5	2	2	1	1	1	1	5	4	4	5	3	5	3	2	1	4	63
B24	1	1	1	1	5	3	5	5	2	2	1	1	1	1	5	4	4	5	4	5	4	3	1	4	69
B25	1	1	1	1	2	3	1	4	2	1	1	1	1	1	5	4	5	5	1	2	3	4	2	3	55
B26	1	1	1	1	2	3	2	5	1	1	1	1	1	1	5	4	5	5	1	3	2	4	2	4	57
B27	1	1	1	1	1	5	2	5	1	1	1	1	1	1	5	5	5	5	1	5	2	2	1	2	56
B28	1	1	1	1	3	3	3	4	1	1	1	1	1	1	5	1	1	5	5	3	2	5	2	5	57
B29	1	1	1	1	3	4	3	5	1	1	1	1	1	1	5	4	5	5	3	3	2	4	2	3	61
B30	1	1	1	1	4	5	1	5	1	1	1	1	1	1	5	4	5	5	2	3	2	4	2	3	60
B31	1	1	1	1	4	2	1	4	1	1	1	1	1	1	5	3	3	5	4	4	2	5	1	5	58
B32	1	1	1	1	5	4	1	5	1	1	1	1	1	1	5	4	5	5	2	4	1	4	1	4	60
B33	1	1	1	1	5	3	3	5	1	1	1	1	1	1	5	2	1	5	4	3	1	4	1	5	57
B34	1	1	1	1	5	3	2	5	1	1	1	1	1	1	5	4	4	5	3	3	1	4	1	4	59

†Meanings of the letters A, Lb, Nu, Rc, Fs, Dd, Si, Rg, Wb, Pr, H, Rr, ReRe, Rn, Rb, Re, Rf, T, Tsi, WMRb, Cc, Rw, HI, and K as they are listed in the table (1)

Table (4): Geomorphometric hazard width values for subdrainage basins in the western Luxor area.

Sub - basin	Hazard Degree†																							Total
	Direct impact													Indirect impact										
	A	Lb	Nu	Rc	Fs	Dd	Si	Rg	Wb	Pr	H	Rr	ReRe	Rn	Rb	Re	Rf	T	Tsi	WMRb	Cc	Rw	HI	K	
B2	4.20	5.00	4.10	2.84	2.44	2.73	4.50	1.08	4.61	3.57	4.70	2.30	1.24	4.62	2.81	4.84	4.94	2.16	3.10	3.45	4.87	2.86	1.07	1.65	78.03
B3	3.52	4.01	3.42	2.77	3.03	2.66	3.86	1.07	4.23	3.24	5.02	2.57	1.37	4.89	1.91	4.54	4.78	2.12	2.81	2.62	4.86	3.87	1.07	1.20	74.24
B4	2.81	2.58	2.89	5.00	1.47	3.38	2.54	1.05	3.76	3.85	4.21	3.26	1.58	4.40	3.41	3.35	3.90	2.72	2.03	3.90	5.00	4.93	1.08	0.48	73.09
B5	1.86	2.83	1.73	1.60	1.73	1.76	3.80	1.23	2.92	1.76	4.25	2.27	1.50	3.81	3.21	4.65	4.84	4.33	2.80	3.66	4.57	2.89	1.06	1.34	65.08
B6	1.86	2.60	1.90	1.77	1.89	3.40	3.39	1.24	2.92	1.86	4.76	2.67	1.68	4.98	3.16	4.39	4.69	4.20	2.57	3.47	4.65	2.76	1.14	1.04	67.92
B7	1.53	2.41	1.52	1.43	2.22	2.72	3.49	1.35	2.52	1.50	2.02	1.42	1.18	2.03	3.28	4.63	4.83	4.48	2.65	3.23	4.44	2.50	1.09	1.31	58.46
B8	1.28	2.26	1.26	1.40	2.44	2.40	2.09	1.58	2.09	1.35	1.88	1.49	1.17	1.86	2.92	4.99	5.01	4.61	1.71	2.97	4.41	1.99	1.07	1.96	54.22
B9	1.23	1.89	1.21	1.64	2.92	2.14	3.00	1.53	1.98	1.40	4.28	3.56	2.06	3.98	3.65	4.58	4.80	4.49	2.42	3.33	4.59	2.89	1.06	1.25	64.65
B10	1.19	2.01	1.17	1.23	2.56	2.13	3.34	1.78	1.88	1.22	4.28	2.70	1.94	3.98	1.00	4.95	4.99	4.75	2.62	1.76	4.16	1.66	1.07	1.88	58.38
B11	1.12	1.63	1.12	1.29	3.10	2.32	2.23	1.78	1.69	1.20	1.40	1.29	1.16	1.41	3.34	4.53	4.77	4.74	1.90	3.58	4.28	2.96	1.04	1.19	53.89
B12	1.12	1.57	1.11	1.39	2.56	2.58	2.37	1.81	1.67	1.22	4.14	3.66	2.55	4.02	3.55	4.43	4.71	4.74	2.02	3.48	4.40	2.89	1.07	1.08	63.06
B13	1.05	1.44	1.05	1.23	2.66	2.79	1.93	2.39	1.42	1.12	3.97	3.80	2.85	3.93	4.17	4.68	4.86	4.86	1.71	4.38	4.16	2.36	1.12	1.39	63.93
B14	1.04	1.11	1.04	1.17	2.99	2.63	5.03	2.55	1.33	1.09	3.35	3.26	5.25	3.29	3.96	1.97	2.38	4.89	3.92	3.43	3.99	2.80	1.15	0.24	63.60
B15	1.03	1.17	1.03	1.04	3.37	2.20	1.64	2.28	1.30	1.04	1.02	1.00	1.07	1.06	3.51	3.27	3.83	4.95	1.60	3.24	2.83	4.00	1.10	0.46	48.58
B16	1.03	1.29	1.04	1.04	3.63	3.53	2.17	2.72	1.29	1.03	1.08	1.03	1.08	1.14	3.51	4.44	4.72	4.95	2.05	3.24	2.76	2.83	1.02	1.10	52.62
B17	1.03	1.32	1.02	1.06	1.42	1.29	3.16	3.45	1.26	1.04	1.14	1.09	1.11	1.14	2.32	4.73	4.88	4.97	2.75	1.00	3.21	1.14	1.03	1.45	46.56
B18	1.02	1.35	1.02	1.38	1.65	2.47	2.91	3.51	1.24	1.11	3.38	5.02	2.81	3.27	3.57	4.93	4.98	4.91	2.58	4.52	4.39	1.01	1.14	1.84	64.17
B19	1.02	1.17	1.02	1.13	3.16	2.59	2.93	2.75	1.21	1.05	1.07	1.10	1.13	1.11	3.96	3.89	4.35	4.93	2.98	3.69	3.80	3.63	1.00	0.69	54.66
B20	1.02	1.15	1.02	1.17	3.57	2.35	1.71	2.52	1.21	1.06	1.08	1.13	1.15	1.11	4.11	3.73	4.22	4.91	1.84	4.33	3.98	4.19	1.12	0.62	53.66
B21	1.01	1.04	1.02	1.04	1.01	3.15	2.77	3.71	1.17	1.02	1.42	1.29	2.35	1.48	4.11	1.32	1.49	4.99	2.67	3.67	2.74	2.05	1.05	0.18	47.56
B22	1.01	1.21	1.01	1.03	1.66	2.30	1.63	3.23	1.15	1.02	1.41	1.28	1.49	1.41	3.66	4.55	4.78	4.99	1.70	3.00	2.63	3.32	1.09	1.21	50.57
B23	1.01	1.15	1.01	1.03	2.78	2.36	3.36	3.71	1.14	1.02	1.09	1.06	1.17	1.12	4.55	4.13	4.52	4.98	3.28	4.77	2.56	2.51	1.04	0.83	55.36
B24	1.01	1.11	1.01	1.10	3.17	1.66	4.06	3.77	1.10	1.03	1.03	1.08	1.12	1.06	4.70	3.95	4.39	4.96	4.10	5.00	3.61	3.00	1.06	0.73	58.08
B25	1.01	1.15	1.01	1.02	2.64	1.38	1.02	3.34	1.10	1.01	0.98	0.99	1.01	1.01	3.66	4.42	4.71	4.99	1.00	3.00	2.20	3.89	1.14	1.07	47.65
B26	1.00	1.11	1.00	1.01	2.70	1.60	1.71	3.72	1.07	1.01	1.36	1.25	1.68	1.33	4.11	4.23	4.59	4.99	2.19	3.67	1.88	3.74	1.07	0.91	52.04
B27	1.00	1.20	1.01	1.01	1.30	4.99	1.84	5.00	1.06	1.01	1.33	1.23	1.42	1.47	5.00	5.00	5.01	5.00	2.00	5.00	1.79	1.96	1.05	1.99	56.68
B28	1.00	1.00	1.00	1.01	3.15	2.02	2.49	3.05	1.05	1.01	1.05	1.03	1.45	1.08	4.11	1.00	1.00	4.99	5.00	3.67	1.69	4.99	1.10	0.16	48.92
B29	1.00	1.11	1.01	1.01	3.28	3.15	2.74	3.93	1.05	1.01	1.05	1.03	1.14	1.09	4.11	4.39	4.69	4.99	3.77	3.67	1.63	3.78	1.09	1.05	55.71
B30	1.00	1.09	1.00	1.01	3.87	4.13	1.63	3.92	1.03	1.00	1.03	1.02	1.14	1.09	4.11	4.24	4.60	4.99	2.54	3.67	1.40	4.09	1.08	0.92	54.68
B31	1.00	1.02	1.00	1.01	2.98	1.01	2.00	3.38	1.03	1.00	1.04	1.03	1.31	1.06	4.55	2.67	3.22	5.00	4.51	4.33	1.34	4.86	1.05	0.33	51.40
B32	1.00	1.08	1.00	1.01	3.29	3.33	1.63	4.28	1.02	1.00	1.08	1.05	1.26	1.13	4.55	4.13	4.52	5.00	2.54	4.33	1.20	3.86	1.00	0.84	54.28
B33	1.00	1.00	1.00	1.00	5.00	2.51	2.63	4.70	1.00	1.00	1.08	1.05	1.58	1.11	4.11	1.92	2.32	4.99	4.18	3.67	0.99	3.61	1.04	0.23	52.47
B34	1.00	1.05	1.00	1.00	5.00	1.60	1.79	4.31	1.00	1.00	1.05	1.03	1.24	1.07	4.11	3.85	4.31	4.99	3.24	3.67	0.98	4.07	1.06	0.67	53.42

† Meanings of the letters A, Lb, Nu, Rc, Fs, Dd, Si, Rg, Wb, Pr, H, Rr, ReRe, Rn, Rb, Re, Rf, T, Tsi, WMRb, Cc, Rw, HI, and K as they are listed in the table (1)

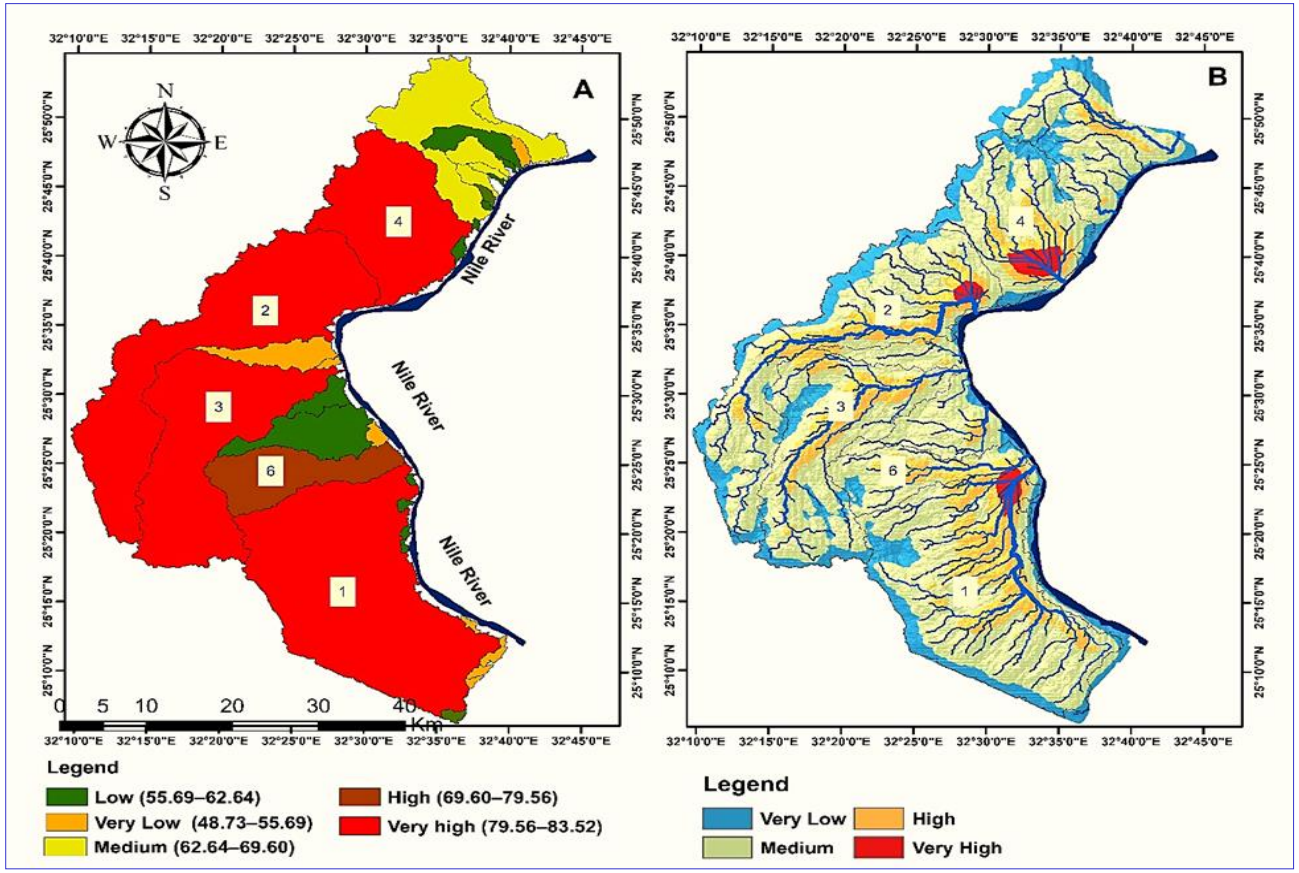

Figure (10): (A) Flash flood potential areas, (B) Overall flash flood potential area.

Table (5): Flood hazard classes located in the western part of the Luxor area.

Class	Calculated Range	Degree of Hazards	Sub-basin number
First	48.73–55.69	Very low	8, 15, 16, 17, 21, 22, 25, 26 and 28
Second	55.69–62.64	Low	7,10, 11, 19, 20, 23, 24, 26, 29, 30, 31, 32, 33 and 34
Third	62.64–69.60	Medium	5,9,12,13,14 and 18
Fourth	69.60–79.56	High	6
Fifth	79.56–83.52	Very high	1, 2, 3 and 4

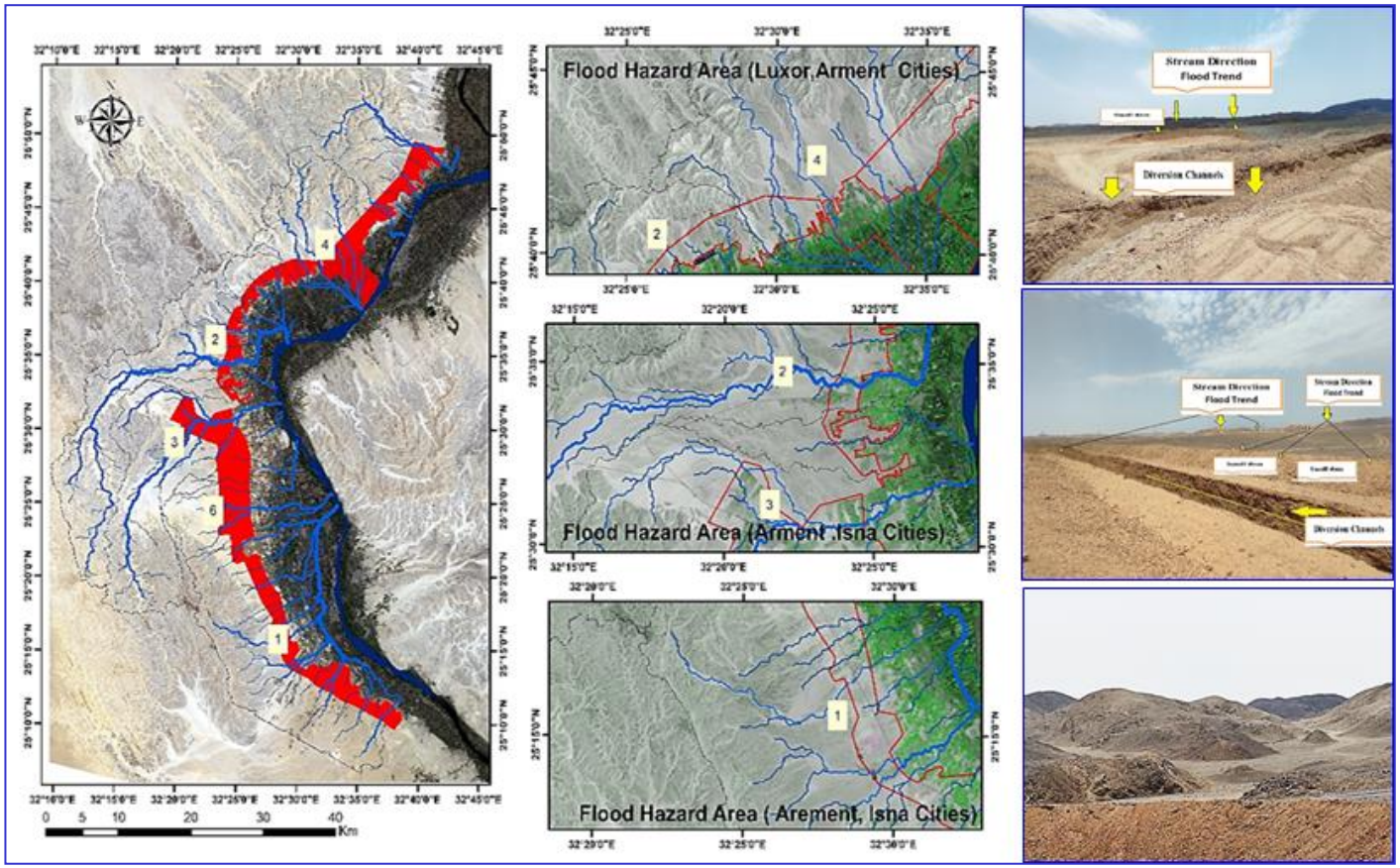

Figure (11): Landsat 8 satellite image showing flood risk areas with Field photographs for the local construction of mitigation measures.

SAN 2020, Quantitative Morphometric Analysis Using Remote Sensing and GIS Techniques for Mandakini River Basi, IOP Conference Series: Earth and Environmental Science, 540:1-10.

ABU EL-MAGD, S.A., ORABI, H.O., ALI, S.A., PARVIN, F., PHAM, Q.P., 2021, An integrated approach for evaluating the flash flood risk and potential erosion using the hydrologic indices and morpho-tectonic parameters. Journal of environmental earth science 80, 694.

ANDREANI, L., STANEK, K., GLOAGUEN, R., KRENTZ, O., DOMÍNGUEZ-GONZÁLEZ, L., 2014, DEM-based Analysis of Interactions between Tectonics and Landscapes in the Ore Mountains and Eger Rift (East Germany and the NW Czech Republic).Journal of Remote Sensing 6: 7971–8001.

ARABAMERI, A., TIEFENBACHER, J.P., BLASCHKE, T., PRADHAN, B., BUI, D.T., 2020, Morphometric Analysis for Soil Erosion Susceptibility Mapping Using Novel GIS-Based Ensemble Model, Journal of Remote Sensing., 12(5):2-24.

ASFAW, D., WORKINEH G., 2019, Quantitative analysis of morphometry on Ribband Gumara watersheds: Implications for soil and water conservation, /International Soil and Water Conservation Research 7:150–157.

BISWAS, S.S., 2016, Analysis of GIS-based morphometric parameters and hydrological changes in Parbati River Basin, Himachal Pradesh, India. Journal of Geographic nature Disasters 6(2): 2-8.

CHEN, C.Y., ANDYU, F.C., 2011, ORPHOMETRIC analysis of debris flows and their source areas using GIS, Journal of Geomorphology, 129: 387–397.

CHOUDHARI, P.P., NIGAM, G.K., SINGH S.K., THAKUR, S., 2018, Morphometric-based prioritization of watershed for groundwater potential of Mula river basin, Maharashtra, India. Journal Geological Ecological Landscape, 2(4): 256-267.

Conoco (1987), Geological Map of Egypt, 1: 500,000, NG36NW-(ASYUT), NG36SW- (LUXOR), NG36NE-(QUSEIR), and NG36SE-(GEBEL HAMATA). The Egyptian Petroleum Cooperation.

DUAN, Y, PEI, X., ZHANG, X., 2022, The Hypsometric Integral Based on Digital Elevation Model for the Area West of Lvliang Mountains in Loess Plateau, Shanxi, China, Journal Frontiers in Earth Science10 (1):1-14.

EBRAHIMI, H., GHAZAVI, R., KARIMI, H., 2016, Estimation of groundwater recharge from the rainfall and irrigation in an arid environment using inverse modeling approach and RS. Journal Water Resource Management 30(6): 1939-1951.

EGSA (Egyptian General Survey Authority) (2006) Egyptian topographic maps, Egyptian series 1:50 000, sheet NG 36 F.

EL- HOSARY, M. F. M., 1994, Hydrogeological and Hydrogeochemical studies on Luxor area, Southern Egypt. M. Sc. Thesis, Faculty Science Menoufia University.

EL SHAMY, I. Z., GAD, M. I., SHEDID, M., EL KAZZAZ, Y.A., AMMAR, M.A.,2013, flash flood estimation in luxor area with emphases on wadi el madamud, south Egypt. the journal of geology 57:103-117

ELEWA, H.H., RAMADAN, M., AND NOSAIR, A.M., 2016, Spatial-based hydro-morphometric watershed modeling for the assessment of flooding potentialities. Journal of Environmental Earth Science 75(10):1-24.

EMRA, (Egyptian Mineral Resources Authority), 2006, GEOLOGICAL MAP OF LUXOR (ALUQSUR) QUADRANGLE, EGYPT, 2006, SCALE 1:100000, NG 36 F6 , MINISTRY OF PETROLEUM.

EMRA, (Egyptian Mineral Resources Authority), 2006, GEOLOGICAL MAP OF ISNA QUADRANGLE, EGYPT, 2006, SCALE 1:100000, NG 36 F3, MINISTRY OF PETROLEUM.

FARHAN, Y., ELGAZIRI, A., ELMAJI, I., AND ALI, I., 2016, Hypsometric Analysis of Wadi Mujib-Wala Watershed (Southern Jordan) Using Remote Sensing and GIS Techniques. International Journal of Geosciences, 7:158-176.

GABALE, S., PAWAR, N., 2015, Quantitative Morphometric Analysis of Ambil Odisha (Rivulet) In Pune, Maharashtra, India. IOSR Journal of Environmental Earth Science. Toxicology Food Technology, 9: 41–48.

GHAREHCHAHI, S., BALLINGER, T. J., JENSEN, J. L. R., BHARDWAJ, A., SAM, L., WEAVER, R. C., 2021, Local- and Regional-Scale Forcing of Glacier Mass Balance Changes in the Swiss Alps. Remote Sensing 13, 1949.

HASSAN, O., 2012, Salient Geo-environmental parameters of Ras Malaab-Abu Zenima Area, Gulf of Suez, Egypt, with an emphasis on flash flood potential and mitigative measures, Egypt, Journal of Remote Sensing Space Science 3:37–58.

HORTON, R.E., 1932, "Drainage basin characteristics". Am. Geophysics Union, 13: 350 – 360.

HORTON, R.E., 1945, Erosional development of streams and their drainage basins; hydro physical approach to quantitative morphology. Geological Society of America Bulletin, 56(3): 275-370.

IQBAL, H.S.M.,2014, Watershed Prioritization using Morphometric and Land Use/Land Cover Parameters of Dudhganga Catchment Kashmir Valley India using Spatial Technology. Journal of Geophysics and Remote Sensing, 3: 1–12.

IVANOVA, E., NEDKOV, R., IVANOVA, I., RADEVA, K., 2012, Morpho-Hydrographic Analysis of Black Sea Catchment Area in Bulgaria. Procedia Environmental Sciences, 14: 143-153.

JHA, V., 1996, Himalayan geomorphology. Rawat publishing Co. Johnson, D. (1933). Available relief and texture of topography a discussion. The Journal of Geology, 41(3): 293–305.

JODAR-ABELLAN, A., VALDES-ABELLAN, J., PLA, C., GOMARIZ-CASTILLO, F., 2019, Impact of land-use changes on flash flood prediction using a sub-daily SWAT model in five Mediterranean ungauged watersheds (SE Spain). Science of the Total Environment, 657:1578-1591.

JOJI, V., NAIR, A., BAIJU, k., 2013, Drainage basin delineation and quantitative analysis of Panamaram Watershedof Kabani River Basin, Kerala using remote sensing and GIS. Journal of Geological Society of India, 82:368–378.

KAMEL, M., 2020, Monitoring of Land Use and Land Cover Change Detection Using Multi-temporal Remote Sensing and Time Series Analysis of QenaLuxor Governorates (QLGs), Egypt Journal of the Indian Society of Remote Sensing, 48(12):1767–1785.

KHARE, D.,2014, Morphometric Analysis for Prioritization using Remote Sensing and GIS Techniques in a Hilly Catchment in the State of Uttarakhand, India. Indian Journal of Science Technology, 7: 1650–1662.

KING, C., DUPUIS, C., AUBRY, M.P., BERGGREN, W.A., KNOX, R.O., GALAL, W.F., BAELE, J.M, (2017), Anatomy of a mountain: the Thebes Limestone Formation (Lower Eocene) at Gebel Gurnah, Luxor, Nile Valley, Upper Egypt. Journal of African Earth Science, 136:61–108.

KUMAR, M., SHARIF, M., AHMED, S., 2017, Flood risk management strategies for the national capital territory of Delhi. India, ISH Journal of Hydraulic Engineering 25(3): 248–259.

KUNTAMALLA, S., NALLA, M., SAXENA, P. R., 2018, Morphometric Analysis of Drainage Basin through GIS: A Case Study from South Western part of Rangareddy District, Telangana State, India, Proceedings of the 11th International Conference on Science, Technology, and Management, Osmania University, Hyderabad, 11–30.

MALIK, S., PAL, S.C.,2020, Is the topography playing a dual role in controlling downstream channel morphology of a monsoon dominated Dwarkeswar River, Eastern India, HydroResearch,3(1): 15-31.

Marafuz, I., Rodrigues, C., Gomes, A.2015, Analysis and assessment of urban flash floods on areas with limited available altimetry data (Arouca, NW Portugal): A methodological approach. Journal of Environmental Earth Science 73: 2937–2949.

MARIJA, L., MARTIN, Z., JORDAN, A., MATTHEW, P., 2022, Rockfall susceptibility and runout in the Valley of the Kings, Journal of Natural Hazards 110, 451–485.

MELTON, M.A.,1958, the Correlation structure of morphometric properties of a drainage system and their controlling agents. Journal of Geology 66:442–460.

MILLER, V.C., 1953, A Quantitative Geomorphic Study of Drainage Basin Characteristics in the Clinch Mountain area, Virginia and Tennessee, Tech. Report. 3, Columbia University, Department of Geology, ONR, Geography Branch, New York. Project NR, 389-042.

MOSSAD, M., EL-GAMMAL, M., EL-ZEINY, A., & GEBRIL, A. (2022). Hydrogeochemical Facies Investigation of Surface and Groundwater Resources at West Luxor Area, Egypt using Spatial and Statistical Techniques. Catrina: The International Journal of Environmental Sciences, 25(1), 27-39. doi: 10.21608/cat.2022.138219.1125-MUELLER, J. E., 1968, An Introduction to the Hydraulic and Topographic Sinuosity Indexes. Annals of the Association of American Geographers, 58(2): 371–385.

NIYAZI, B., ZAIDI, S., MASOUD, M., 2019, Comparative Study of Different Types of Digital Elevation Models based on Drainage Morphometric Parameters (Case Study of Wadi Fatimah Basin, KSA). Journal Earth Systems and Environment, 3: 539–550.

PANGALI SHARMA, T.P., ZHANG, J., KHANAL, N.R., PRODHAN, F.A., NANZAD, L., ZHANG, D., NEPAL, P. A., 2021, Geomorphic Approach for Identifying Flash Flood Potential Areas in the East Rapti River Basin of Nepal. ISPRS International Journal of Geo-Information, 10(4):247.

RAI, P.K., MISHRA, V.N., AND MOHAN, K., 2017, A study of morphometric evaluation of the Son basin, India using the geospatial approach. Remote Sensing Applications: Society and Environment. 7: 9-20.

RAI, P.K., SINGH, P., MISHRA, V.N., SINGH, A., SAJAN, B., SHAHI, A.B., 2019, Geospatial approach for quantitative drainage morphometric analysis of Varuna river basin, India, Journal of Landscape Ecology, 12 (2):1-25.

RANA, N.K., 2018, Analysis of Mahananda River Basin Using Geospatial Data. The Indian Rivers, Springer, Singapore, 239-250.

SANGMA, F., GURU, B., 2020, Watersheds characteristics and prioritization using morphometric parameters and fuzzy analytical hierarchal process (FAHP): a part of the lower Subansiri sub-basin. Journal of the Indian Society of Remote Sensing,48: 473–496.

SCHUMM, S.A., 1956, Evolution of drainage systems and slopes in badlands at Perth Amboy, New Jersey. Geological Society of America Bulletin, 67(5): 597-646.

SHAH, M.A.R., RAHMAN, A., CHOWDHURY, S.H., 2018, Challenges for achieving sustainable flood risk management. Journal Flood Risk Manag 11:S352–S358.

SHARMA, S., MAHAJAN, A.K., 2020, GIS-based sub-watershed prioritization through morphometric analysis in the outer Himalayan region of India. Applied Water Science 10:163.

SHIVASWAMY, M., RAVIKUMAR, A.S., SHIVAKUMAR, B.L., 2019, Quantitative Morphometric and Hypsometric Analysis Using Remote Sensing and G.I.S. Techniques. International Journal of Advanced Research in Engineering and Technology 10: 1–14.

SINGH, A.P., ARYA, A.K., SINGH, D.SEN, 2020, Morphometric Analysis of Ghaghara River Basin,

India, Using SRTM Data and GIS. Journal of Geological Society of India. 95, 169–178.
SMART, J.S., SURKAN, A.J., (1967), The relation between mainstream length and area in drainage basins. Water Resources 3(4):963–973.
STRAHLER, A.N., 1952, Hypsometric (Area-Altitude) Analysis of Erosional Topography. Geological Society of America Bulletin, 63: 1117-1141.
STRAHLER, A.N., 1957, Quantitative analysis of watershed geomorphology. Trans Am Geophysics Union, 38:913–920.
STRAHLER, A.N.,1964, Quantitative Geomorphology of Drainage Basin and Channel Networks. In: Chow, V.T., Ed., Handbook of Applied Hydrology, McGraw-Hill, New York, 439-476.
TESEMA, T.A., 2021, Impact of identical digital elevation model resolution and sources on morphometric parameters of Tena watershed, Ethiopia, Journal of Heliyon,7,1-9.

رسم خرائط لمخاطر الفيضانات في غرب الأقصر ، مصر باستخدام الاستشعار من البعد والتحليلات المكانية

محمد جبريل [1]، مى الجمال [2] ، احمد الزينى [3]، مرفت السنباطى[1]

[1] قسم العلوم البيئية، كلية العلوم، جامعة دمياط، دمياط، مصر
[2] قسم الدراسات البيئية ،الهيئة القومية للأستشعارمن البعد وعلوم الفضاء،القاهرة، مصر
[3] قسم الدراسات الجيوكيميائية ،المعامل المركزية، الهيئة المصرية العامة للثروة المعدنية، الجيزة، مصر

الملخص العربــي

إدارة مستجمعات المياه أمر بالغ الأهمية للتنمية المستدامة ، تؤدي الظروف الطبوغرافية والهيدروجيومورفولوجية في الجانب الغربي من منطقة الأقصر إلى حدوث فيضانات مفاجئة. يتم التوسع الزراعى والعمرانى فى المنطقة الصحراوية غرب الأقصر بطريقة عشوائية غير منظمة ويتجة باتجاه الهضبة الهيكلية الغربية وهذه المناطق في مواجهة مباشرة مع مخاطر الفيضانات المفاجئة. الغرض من هذه الدراسة هو رسم خريطة لمخاطر الفيضانات للجانب الغربي من منطقة الأقصر بأستخدام ، 1- نموذج مؤشر مستجمعات المياه الخطي (LWIM) بتعريف وتحليل عدد 24 من المعاملات المورفومترية ، 2- نموذج DEM كمدخل في بيئة نظم المعلومات الجغرافية باستخدام اداةArc-Hydro 3 .دمج انظمة الاستشعار من البعد والمعلومات الجغرافية للكشف عن LU/LCمن خلال التصنيف الإشرافى الموجه للصور Landsat لعامى 1991و 2021، وتحديد كثافة مناطق التصريف. تشير النتائج الى زيادة فى مساحة الأراضى الزراعية بنحو (292.7 كم2)، بينما زاد العمران بمقدار (43 كم^2) بين عامى 1991و2021. وخلصت هذه الدراسة إلى أن مناطق الفيضانات غرب الأقصر محصورة في المنطقة الصحراوية غرب مدن الأقصر ، أرمنت و إسنا، وتمثل هذه المناطق 13.25٪ من المناطق المعرضة لمخاطر الفيضانات. اقترحت الدراسة إنشاء سدود صغيرة مع قنوات تحويل في طريق القنوات الرئيسية ذات الرتب العالية 4 و 5 و 6 وتوجية مياه الفيضانات إلى قنوات جديدة والتى تقوم بتوجية المياة إلى القنوات الرئيسية في منطقة الدراسة، كذلك اعادة تخطيط المنطقة الصحراوية غرب مدينة الاقصر.